REGULAR PAPER

New Deconvolution Method for Electrospray Ionization Mass Spectrometry

Hiroshi KATO,*[a] Morio ISHIHARA,[b] and Munetaka NAKATA[c]

(Received August 14, 2000; Accepted October 11, 2000)

A new method is proposed for elimination of artifacts appearing in deconvolution of electrospray ionization mass spectra, where two algorithms, a partial correlation method (PCM) and a sub-harmonic artifact removal filter (SHARF), are used. In addition to the elimination of artifacts, the former algorithm removes influence of singly charged ions generated from contamination in a sample, while the latter algorithm removes influence of background noises and baseline offsets in a measured spectrum. The proposed method results in supplying the deconvoluted spectra free from artifacts with good signal-to-noise ratios and without distortion on peak shapes. Applications to some bio-molecules lead to the conclusion that our method is especially useful for analyses of their mixture samples, which show complicated mass spectra.

1. Introduction

Electrospray ionization (ESI) has been one of the most indispensable methods in biological mass spectrometry,[1] since it was firstly applied to bio-molecules by Fenn *et al.*[2] The mass spectra generally consist of a coherent sequence of peaks due to multiply charged ions produced by ESI, with smaller intervals at lower mass-to-charge ratios (m/z) and typically with an intensity envelope nearly like Gaussian distribution. Although this feature seems to complicate mass spectral interpretation, an accurate mass of the parent molecule can be determined from the sequence of peaks measured by even a conventional mass spectrometer with the limited m/z range, if suitable algorithms are adopted.

The averaging algorithm[3,4] is widely used in the mass determination by ESI mass spectrometry, where at least two multiply charged ions must be identified. The identification, however, is difficult for spectra that contain many peaks of singly charged ions due to contamination in a sample and/or multiply charged ions of different components in a mixture sample. Then, another method, deconvolution algorithm, was proposed by Mann *et al.*,[4] who transformed the peaks of multiply charged ions to one singly charged peak located at the mass of a parent molecule, M_0. Although the Mann method is simple, spurious peaks called artifacts are simultaneously produced around the true peak at M_0 in the deconvoluted spectrum. The artifacts sequentially appearing at $2M_0$, $3M_0$, $4M_0$, $\cdots$ are here called harmonic artifacts, while the artifacts appearing at $M_0/2$, $M_0/3$, $M_0/4$, $\cdots$ are called sub-harmonic artifacts, the harmonic artifacts of which also appear in the deconvoluted spectrum.

For the elimination of these artifacts, a couple of studies[5,6] have been reported. However, there has been no effective way to eliminate all the artifacts until now; for example, the mutiplicative algorithm proposed by Hagen and Monning[6] eliminates sub-harmonic artifacts, but does not harmonic artifacts. All the artifacts in the deconvoluted spectra with resolution enhancement may be possibly eliminated by a maximum-entropy method[7,8]; however, it consumes a lot of time in the calculation. Recently, Zhang *et al.* have reported a new algorithm based on a charge scoring scheme.[9] Although all the artifacts can be eliminated by their method, the identification of peaks is ambiguous when they heavily overlap with other peaks generated by different components in a mixture sample. If ultra-high resolution instruments such as a Fourier-transform mass spectrometer (FTMS) are available, the information on isotope species may be useful to decrease the ambiguity.

In the present study, we propose a new method to eliminate the artifacts in deconvoluted spectra derived from data measured with a conventional mass spectrometer without any information on isotopically resolved peaks. The algorithms used here consist of a partial correlation method (PCM) and a sub-harmonic artifact removal filter (SHARF). It is demonstrated that our method supplies the deconvoluted spectra free from artifacts for some bio-molecules and their mixture samples, which show complicated mass spectra.

2. Theory

Before the explanation of our algorithms, the deconvolution procedure and the generation mechanism of artifacts are described with the effective and simple deconvolution calculation.

2.1 Deconvolution

The following relationship between a molecular mass (M) and the observed m/z (m_i) of the multiply charged ion with a charge number (i) is held in trans-

*[a] *JEOL Ltd. (3-1-2 Musashino, Akishima, Tokyo 196-8558, Japan)*
[b] *Department of Physics, Graduate School of Science, Osaka University (1-16 Machikaneyama, Toyonaka, Osaka 560-0043, Japan)*
[c] *Graduate School of Bio-Applications and Systems Engineering, Tokyo University of Agriculture and Technology (2-24-16 Naka-cho, Koganei, Tokyo 184-8588, Japan)*

formation of deconvolution,

$$m_i = \frac{M}{i} + m_a , \tag{1}$$

where m_a represents the mass of an adduct ion. An intensity of a deconvoluted spectrum ($I_M(M)$) is calculated from the intensities of a measured spectrum ($I_m(m_i)$) at m_i appearing in Eq. (1) with different charge numbers (i). In the Mann method, for example, the intensity ($I_M(M)$) is given by a sum of the intensities ($I_m(m_i)$),

$$I_M(M) = \sum_i I_m(m_i) . \tag{2}$$

This calculation must be performed at every M in an interesting range of the molecular mass axis to deconvolute the measured spectrum. Thus, the computational time for the extraction of the intensities ($I_m(m_i)$) is dominant in the deconvolution calculation. One can extract them simply and efficiently, if measured and deconvoluted spectra are expressed in terms of new variables, s and t, respectively, defined as

$$s \equiv \frac{1}{m - m_a} = \frac{i}{M} \tag{3}$$

and

$$t \equiv \frac{1}{M} , \tag{4}$$

where m is used instead of m_i for expression of the m/z axis of a measured spectrum ($I_m(m)$). A spectrum ($I_s(s)$) can be calculated from $I_m(m)$ by using the new parameter (s):

$$I_s(s) = I_m\left(\frac{1}{m - m_a}\right) . \tag{5}$$

It is noted that the multiply charged ions in $I_s(s)$ appear in the reverse order of those in $I_m(m)$ and a difference between adjacent multiply charged ions at s_i and s_{i+1} is equal to $1/M$.

$$s_{i+1} - s_i = \frac{i+1}{M} - \frac{i}{M} = \frac{1}{M} = t . \tag{6}$$

Figure 1 shows that multiply charged ions of the molecular mass (M_0) appear at the constant intervals of $1/M_0 = t_0$ in $I_s(s)$, while they appear at decreasing intervals in $I_m(m)$ with increases of their charge numbers.

For convenience, a discrete function (U) is introduced to express the intensities at intervals of t, defined in Eq. (4), in $I_s(s)$.

$$U(t, i) = I_s(it) . \tag{7}$$

Three examples of U are shown in Fig. 1. The U elements are effectively and simply obtained by extracting the intensities ($I_s(s)$) at multiples of t. A deconvoluted spectrum ($I_t(t)$) can be derived from the $U(t, i)$ elements. In the Mann method, for example, an intensity of $I_t(t)$ is a sum of the $U(t, i)$ elements,

$$I_t(t) = \sum_i U(t, i) . \tag{8}$$

Equation (8) essentially corresponds to Eq. (2). The final deconvoluted spectrum ($I_M(M)$) is derived from $I_t(t)$,

$$I_M(M) = I_t(1/t) . \tag{9}$$

It is noted that the peaks in $I_t(t)$ appear in the reverse

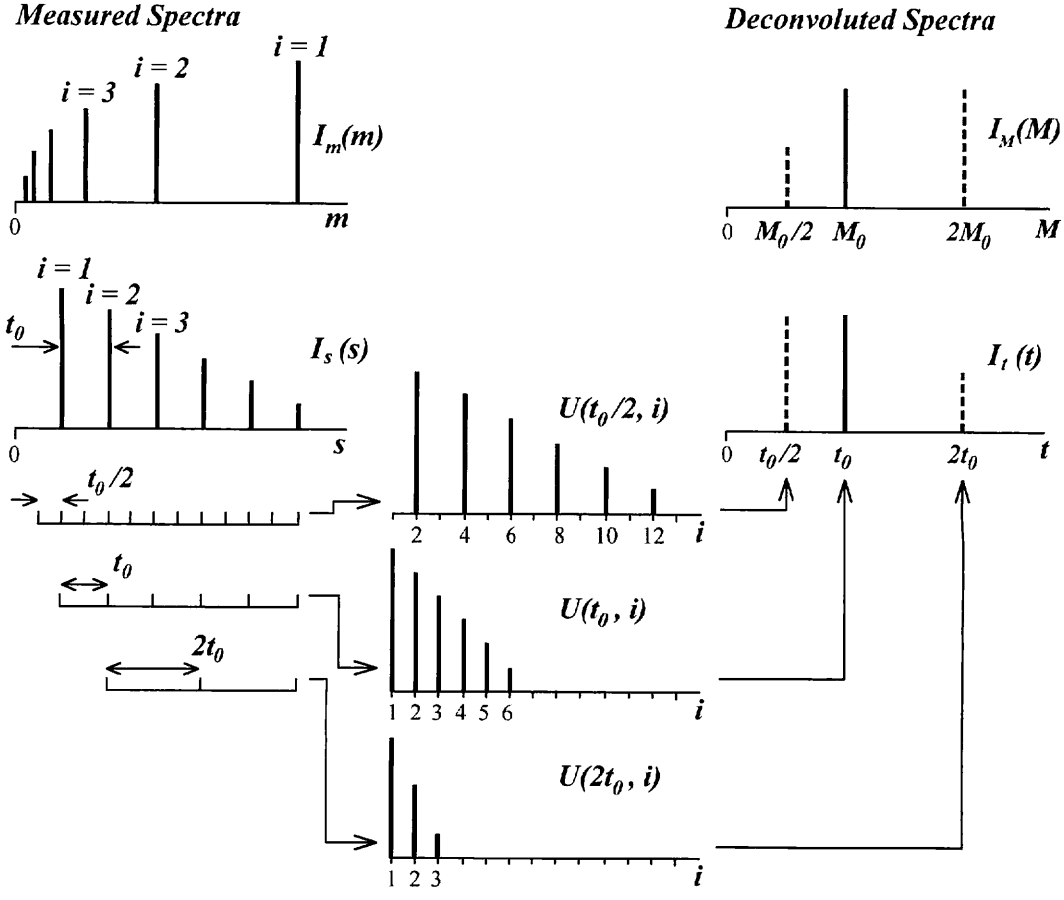

Fig. 1. Schematic diagram of a deconvolution calculation for multiply charged ions generated from the molecular mass of M_0. Their peaks are shown without widths, and with smaller heights as increasing the charge numbers.

order of those in $I_M(M)$. Since $U(t, i)$ extracted from $I_s(s)$ with t play an important role in the artifact elimination, $I_s(s)$ and $I_t(t)$ are treated as a measured spectrum and its deconvoluted spectrum, respectively, instead of $I_m(m)$ and $I_M(M)$, hereafter.

2.2 Artifact

Figure 1 shows three examples of U, the intensities of which are represented with the abscissa of the element numbers. Among these U, the intensities of the $U(t_0, i)$ elements are derived from those of peaks at multiples of t_0 in $I_s(s)$. Since the multiply charged peaks shown in Fig. 1 appear at multiples of t_0 in $I_s(s)$, they are consecutively extracted into $U(t_0, i)$ with the element numbers corresponding to the charge numbers of the multiply charged ions. The intensities of the multiply charged ions are transformed to the true deconvoluted peak at t_0 in $I_t(t)$ by summing all the $U(t_0, i)$ elements, if the Mann method is used. However, the simple summation generates artifacts because the intensities of the multiply charged ions also appear in the other examples of $U(t_0/2, i)$ and $U(2t_0, i)$.

The intensities of the $U(t_0/2, i)$ elements are derived from those of the peaks at multiples of $t_0/2$ in $I_s(s)$ so that the multiply charged ions in $I_s(s)$ appear in $U(t_0/2, i)$ with the element numbers $2i$. Thus, the simple summation generates the harmonic peak at $t_0/2$ with the same intensity of the true peak at t_0 in $I_t(t)$. Similarly, other harmonic artifacts of higher orders also appear at $t_0/3$, $t_0/4$, and so on. Furthermore, the intensities of the $U(2t_0, i)$ elements are derived from those of peaks at multiplies of $2t_0$ in $I_s(s)$ so that the multiply charged ions with charge number $2i$ appear in $U(2t_0, i)$. The summation of the $U(2t_0, i)$ elements causes the sub-harmonic peak at $2t_0$ with a nearly half intensity of the true peak at t_0 in $I_t(t)$. Similarly, other sub-harmonic artifacts of higher orders appear at $3t_0$, $4t_0$, and so on. Their intensities decrease with increases of the orders, because the number of artifact intensities appearing in U decreases.

In generally speaking, harmonic artifacts appearing at t_0/n are generated by harmonic intensities in $U(t_0/n, i)$, and sub-harmonic artifacts appearing at nt_0 are generated by sub-harmonic intensities in $U(nt_0, i)$, where n represent integers larger than one. A suitable algorithm is necessary for elimination of artifacts intensities such as $U(t_0/2, i)$ and $U(2t_0, i)$ and for transformation of the true intensities of $U(t_0, i)$ to $I_t(t_0)$ in order to obtain a deconvoluted spectrum free from the artifacts.

2.3 Partial correlation method

To eliminate the harmonic artifacts, we have developed a partial correlation method (PCM). A deconvolution algorithm for elimination of the artifacts essentially works as a filter that suppresses artifact intensities in U and transfers the true intensities in U to $I_t(t)$ as much as possible. To accomplish this, we introduce a filter function (Ψ) that produces an output from more than two elements of U with consecutive element numbers (i),

$$\Psi(t, i)=\Psi(U(t, i), U(t, i+1), \cdots, U(t, i+N-1)) \quad (10)$$

where N is the number of U elements used for the calculation of one Ψ value and is called a PCM order. Ψ can eliminate the harmonic artifact intensities not appearing consecutively in the U elements by using a correlation among partially selected N elements of U and by reflecting the smallest intensity in these U elements. Then, the deconvolution spectrum free from the harmonic artifacts can be obtained by summation of the Ψ values instead of the U elements,

$$I_t(t)=\sum_i \Psi(t, i). \quad (11)$$

Figure 2 shows two different sequences of multiply charged peaks with the intervals of t_0 and of $2t_0$; the former sequence is transformed to the true peak at t_0, and the latter is transformed to the harmonic artifact at t_0 by the Mann method. It is noted that true and artifact intensities are transformed at the same t_0 from two different sequences in Fig. 2 whereas true and artifact intensities are transformed at different t from one sequence in Fig. 1. With the sequences in Fig. 2, the work of Ψ is explained by using a minimum function, which outputs the smallest value in the selected N elements of U. For example, the minimum function for Ψ with the PCM order of 2 outputs a smaller intensity in the two selected U elements. In Fig. 2a, $\Psi(t_0, 1)$ leads to $U(t_0, 2)$ because $U(t_0, 2)$ is smaller than $U(t_0, 1)$, $\Psi(t_0, 2)$ leads to $U(t_0, 3)$, and so on. Then, the values of $\Psi(t_0, i)$ are corresponding to the intensities of $U(t_0, i+1)$. Thus, the intensities of the sequence with the intervals of t_0 are transformed to the true peak at t_0 in $I_t(t)$, except the intensity of $U(t_0, 1)$. In Fig. 2b, on the other hand, all the values derived from Ψ are zero because either intensity of the selected two elements of U is zero. Thus, the intensities of the sequence with the intervals of $2t_0$ are not transformed to the artifact peak at t_0 in $I_t(t)$; therefore, the artifact intensity at t_0 disappears in $I_t(t)$. Although the minimum function can satisfactorily eliminate the harmonic artifacts, it has a disadvantage that the most intense U element such as $U(t_0, 1)$ shown in Fig. 2a is ignored in transformation to the true peak.

Other suitable algorithms for Ψ are found in the

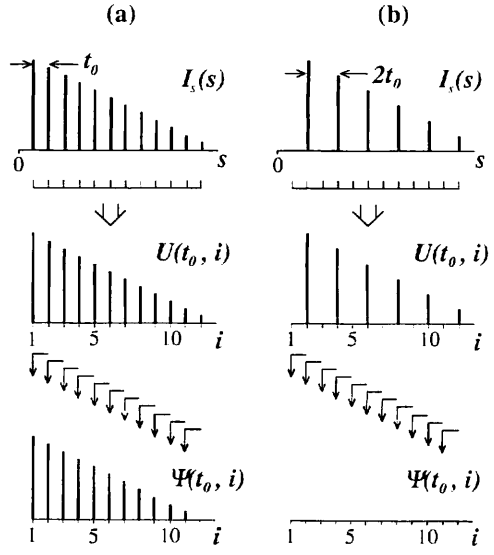

Fig. 2. PCM of the harmonic artifact elimination at t_0 applied to multiply charged ions appearing at intervals of t_0 in $I_s(s)$, and to ones appearing at intervals of $2t_0$ in $I_s(s)$.

averaging calculations, such as geometric and harmonic means. An arithmetic mean is one of the averaging calculations, but it is not good for Ψ because its summation gives the same result as the Mann method. On the other hand, the calculations of geometric and harmonic means are good for Ψ because their results reflect the smallest intensity in the selected U elements. Additionally, the feature that they use all U elements in transformation to the true peaks is an advantage over the minimum function described above. It is found that the harmonic mean is more effective for the artifact elimination than the geometric mean, judging from the fact that the former value is smaller than the latter value. The harmonic mean is therefore used as Ψ, which is expressed as

$$\Psi(t, i)=\sum_{j=i}^{i+N-1}\frac{N}{1/U(t, j)}. \qquad (12)$$

In addition to the harmonic artifact elimination, Ψ effectively works to eliminate the intensities accidentally included in U elements. These noise intensities in U elements originate from singly charged ions due to contamination in a sample and/or multiply charged ions due to different components in a mixture sample. Since these intensities appear in U elements not with consecutive but with sprinkling element numbers, the noise intensities are removed by the function of Ψ. Furthermore, PCM with a large PCM order can remove the intensities of sub-harmonic artifacts since the number of sub-harmonic intensities appearing in U is rather smaller than that of the corresponding true intensities. For example, the sub-harmonic artifact at $2t_0$ caused by three artifact intensities in $U(2t_0, i)$ shown in Fig. 1 is eliminated by PCM with the order of 4. However, an increase of the PCM order to eliminate sub-harmonic artifacts is not adequate because it may also remove the true peaks transformed from a small number of multiply charged peaks.

2.4 Sub-harmonic artifact removal filter

To overcome the situation mentioned above, we have developed an additional algorithm, a sub-harmonic artifact removal filter (SHARF). SHARF uses $U(t_0/n, i)$ to remove the sub-harmonic artifacts appearing at t_0 in $I_t(t)$. Figure 3 shows examples of the SHARF calculation with $n=2$, where two different sequences of multiply charged peaks with the intervals of t_0 and $t_0/2$ are represented; the former sequence is transformed to the true peak at t_0, while the latter is transformed to the sub-harmonic artifact at t_0 by the Mann method.

In the SHARF calculation, $U_0(t_0/2, i)$ and $U_1(t_0/2, i)$ are newly derived from $U(t_0/2, i)$: $U_0(t_0/2, i)$ and $U_1(t_0/2, i)$ correspond to $U(t_0/2, 2i)$ and $U(t_0/2, 2i-1)$, respectively, as shown in Fig. 3. A comparison of them shows that the intensity contributions of both U_0 are similar but those of U_1 are different: no intensities of U_1 are present in Fig. 3a, whereas the intensity distribution of U_1 is similar to that of U_0 with consecutive element numbers in Fig. 3b. For measurement of the difference between U_0 and U_1, new values of I_0 and I_1 are calculated from U_0 and U_1, respectively, using the PCM calculation that removes the influence of noise intensities accidentally included in U. The PCM order used in the I_0 and I_1 calculations is half of that used in the harmonic elimination, because an intensity distribution of each

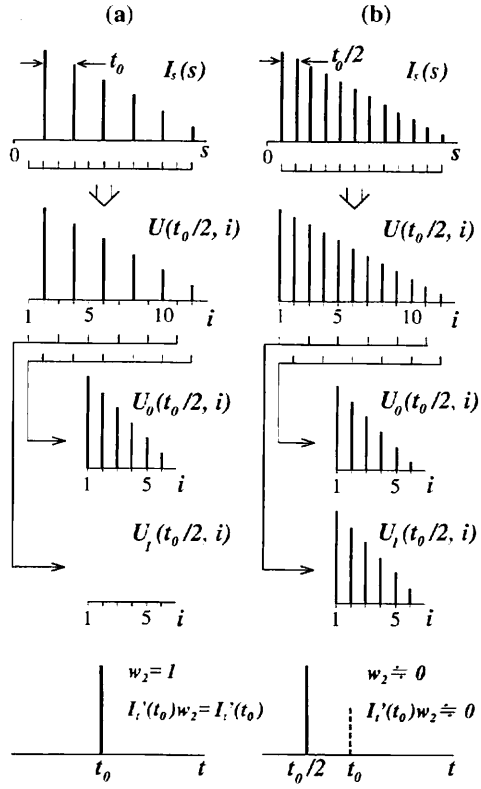

Fig. 3. SHARF of the sub-harmonic artifact elimination at t_0 applied to multiply charged ions appearing at intervals of t_0 in $I_s(s)$, and to ones appearing at intervals of $t_0/2$ in $I_s(s)$.

U_0 and U_1 is reduced to a half of one of $U(t_0/2, i)$. Using I_0 and I_1, we define a weight factor (w_2), which is limited in the range between 0 and 1.

$$w_2=(I_0-I_1)/I_0. \qquad (13)$$

The value of w_2 becomes larger with an increase of the difference between U_0 and U_1. $I_t(t_0)$ is derived from w_2 and $I_t'(t_0)$ that results in the harmonic artifact elimination by PCM.

$$I_t(t_0)=I_t'(t_0)w_2. \qquad (14)$$

In Fig. 3a, for example, w_2 is one since no intensities in U_1 lead I_1 to zero. Thus, $I_t(t_0)$ is equal to $I_t'(t_0)$, where SHARF preserves the true intensity calculated by PCM. In Fig. 3b, on the other hand, w_2 is nearly equal to zero, since the similar intensity distributions between U_1 and U_1 lead I_1 to nearly I_0. Thus, the sub-harmonic intensity at t_0 is removed by SHARF.

For the elimination of the third order sub-harmonic artifacts, another weight factor (w_3) is calculated from the pair of $U_0(t_0/3, i)$ and $U_1(t_0/3, i)$ that are derived from $U(t_0/3, i)$: $U_0(t_0/3, i)$ and $U_1(t_0/3, i)$ correspond to $U(t_0/3, 3i)$ and $U(t_0/3, 3i-1)$, respectively. The PCM order used in the I_0 and I_1 calculations is 3-fold smaller than that used in the harmonic elimination, because an intensity distribution of each U_0 and U_1 is reduced to one-third of one of $U(t_0/3, i)$. The other weight factors for the higher orders such as w_5 and w_7 can be calculated as well as w_3. In this study, we take the weight factors up to w_5 into account to obtain the final deconvoluted spectrum,

$$I_i(t)=I'_i(t)w_2w_3w_5\,. \qquad (15)$$

SHARF using Eq. (15) removes almost the sub-harmonic artifacts arising from the multiply charged peaks with intervals of t_0: w_2 works to remove the artifacts at $2t_0, 4t_0, \cdots$, w_3 does at $3t_0, 6t_0, \cdots$, and w_5 does at $5t_0, 10t_0 \cdots$. The other sub-harmonic artifacts such as $7t_0, 11t_0$, and $13t_0$ are removed not by SHARF but by PCM, because the number of their artifact intensities appearing in U becomes considerably smaller than that of the true intensities.

3. Experimental

Bovine heart cytochrome *c*, horse heart myoglobin and hen egg lysozyme were purchased from Sigma Corp. (St, Louis, MO, U.S.A) and were used without further purification. Ultramark 1621 was obtained from PCR Inc. (Florida, U.S.A). A JMS-700 double focusing magnetic sector type mass spectrometer equipped with an electrospray ionization source (JEOL Ltd., Tokyo, Japan) was operated with the accelerating voltage of 5 kV, the ring voltage of 100 V, and the needle potential of 2 kV. Samples were introduced into an electrospray interface by the flow injection method, with a mobile phase of 70% methanol and 30% water containing 0.2% acetic acid, at the flow rate of 50 microliter/min. Programs for our method and for the Mann method were developed by a Borland Delphi 2.0 compiler on a Microsoft Windows NT operating system running on a computer with an Intel Pentium II 400 MHz microprocessor.

4. Results and Discussion

For evaluations of PCM and SHARF, a synthetic spectrum with multiply charged ions of the molecular mass $M_0=16{,}950$ was used. Figure 4a shows the spectrum, where an intensity distribution of the multiply charged ions is assumed to be Gaussian with the maximum at the charge number of 21, and their peak profiles are to be Gaussian in a resolution of 500. Figure 4b shows the corresponding deconvoluted spectrum obtained by using the Mann method. As shown in Fig. 4c, PCM with the order of 3 eliminates most artifacts appearing in the result of the Mann method, except for sub-harmonic artifacts. Furthermore, the intensities of the sub-harmonic artifacts are so small that they are hardly detected in the result of PCM with SHARF (Fig. 4d). It is concluded that the harmonic artifacts in the synthetic spectra are completely eliminated by even PCM with the order of 2. SHARF weakens the intensities of the sub-harmonic artifacts to be less than 1% of the true peak, except for the artifact at $M_0/7$; it is eliminated by PCM with the order of 3, as described in the theory section.

PCM and SHARF were applied to an actually measured spectrum of cytochrome *c*, shown in Fig. 5a. The deconvoluted spectrum of the Mann method is also shown in Fig. 5b to be compared with our results. Although PCM with the order of 3 removes harmonic artifacts (Fig. 5c) and SHARF removes sub-harmonic artifacts (Fig.5d), the peak at $2M_0$ still remains with a small intensity in both the results. Judging from the fact that PCM completely eliminates the intensity of

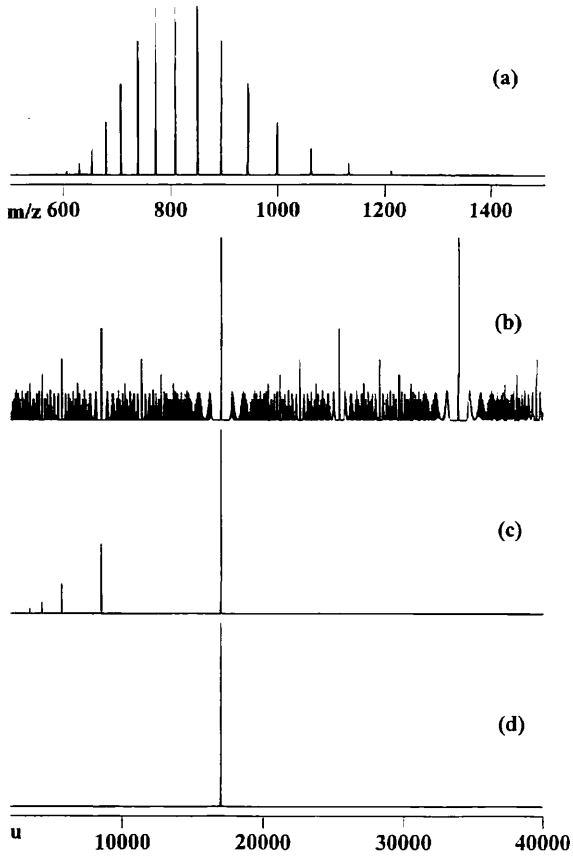

Fig. 4. Deconvolution applied to a synthetic spectrum with multiply charged ions of the molecular mass $M_0=16{,}950$: (a) synthetic spectrum, (b) its deconvoluted spectrum calculated by the Mann method, (c) one by PCM only, and (d) one by PCM with SHARF.

the harmonic artifact at $2M_0$ in the synthetic spectra, this small peak is not considered to be an artifact but a true peak. It probably arose from cytochrome *c* dimerized in the measurement.[10]

Computational times for the deconvolution in Fig. 5 are 1, 2, and 6 seconds for the Mann method, PCM only and PCM with SHARF, respectively, on a computer with a Pentium II 400 MHz processor. Data points of the spectra are 19,322 and 52,754 for the measured spectrum with the *m/z* range from 500 to 2,000 and for the deconvoluted spectra with the molecular mass range from 2,000 to 30,000, respectively. The effective algorithm extracting intensities of a measured spectrum enables us to accomplish such high-speed computation. The result of PCM with SHARF shows smaller background noises and a flatter baseline than the other results. In the Mann method and PCM, intensities of their deconvoluted spectrum are sums of either U elements or Ψ values. The larger M of the deconvoluted spectrum, the larger number of U elements or Ψ values is used for the summation. Even small baseline offsets and background noises, large influence appears in $I_M(M)$ when M becomes large. As a result, the deconvoluted spectrum shows a gradually raised baseline and larger noises with an increase of M. This trend is slightly observed in Figs. 5b and 5c, but not in Fig. 5d

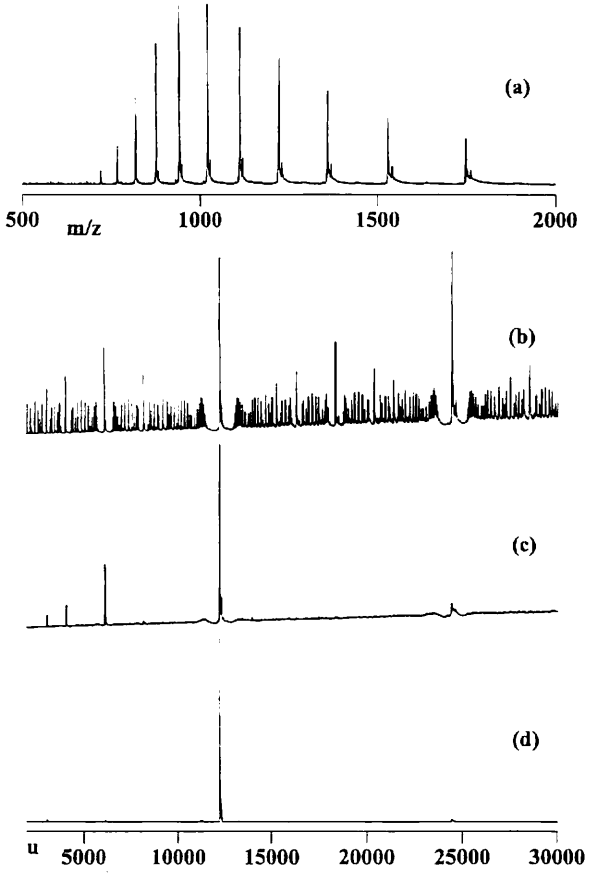

Fig. 5. Deconvolution applied to an actually measured spectrum of cytochrome *c*: (a) measured spectrum, (b) its deconvoluted spectrum calculated by the Mann method, (c) one by PCM only, and (d) one by PCM with SHARF.

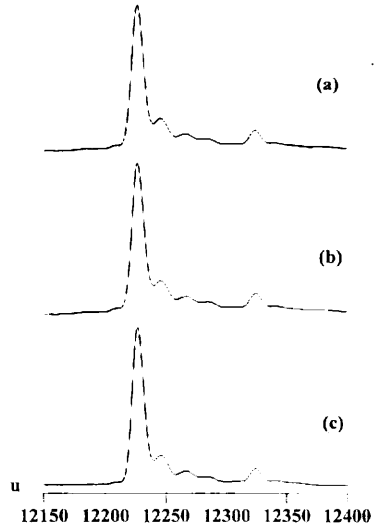

Fig. 6. Expanded spectrum of Fig. 5 for a comparison of peak shapes: (a) deconvoluted spectrum calculated by the Mann method, (b) one by PCM only, and (c) one by PCM with SHARF.

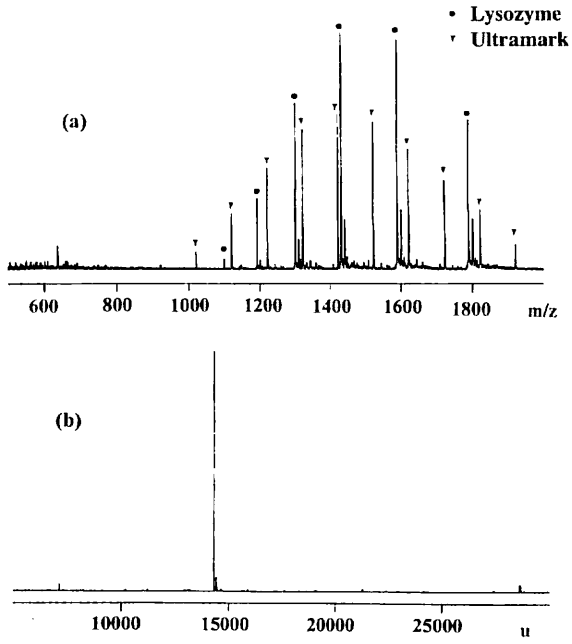

Fig. 7. Analysis of a spectrum complicated with singly charged ions: (a) measured spectrum of lysozyme with contamination of Ultramark, and (b) its deconvoluted spectrum calculated by PCM with SHARF.

of the result with SHARF. As mentioned in the theory section, the weight factors of SHARF represent the dissimilarity of intensity distributions between U_0 and U_1, the intensities of which are alternately extracted from the corresponding U. Since baseline offsets are constant and background noises fluctuate over the measured m/z range, both U_0 and U_1 include the offsets and the noises with the same degree; namely, intensities of the offsets and the noises in U_0 and U_1 contribute to the similarity between U_0 and U_1, but not to the dissimilarity. Thus, they are canceled in the calculations of the weight factors even when M is large. Consequently, SHARF supplies the deconvoluted spectrum with a flat baseline and a good signal-to-noise ratio.

Although the Mann method generates many artifacts, its deconvolution of the simple summation of measured intensities preserves the original peak shape. On the other hand, a deconvolution algorithm with non-linear calculation is accompanied with peak distortion as a sacrifice of artifact elimination.[6] Figure 6 shows the expanded spectra around the molecular mass of cytochrome *c* in Fig. 5; there are a main peak of cytochrome *c* due to proton adduction and small peaks due to sodium, potassium and other adduct ions.[11] By comparing the spectra in Fig. 6 each other, the spectra calculated by our method are almost the same as that by the Mann method. Although our method uses the non-linear calculation such as the harmonic mean, it preserves the peak shapes to be comparable to the Mann method.

PCM and SHARF effectively work for complicated spectrum patterns composed of singly charged ions and/or of multiply charged ions generated by more than one molecular mass. For example, protein samples sometimes contain surface active agents as contamination such as polyethylene glycol; this produces singly charged ions with equal m/z intervals and with a similar intensity distribution of multiply charge ions.

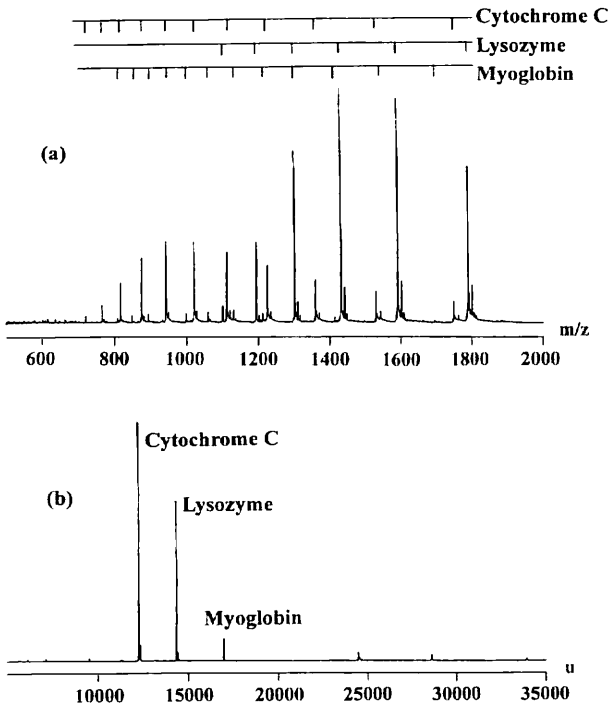

Fig. 8. Analysis of a spectrum complicated with multi-components: (a) measured spectrum with cytochrome *c*, lysozyme, and myoglobin, and (b) its deconvoluted spectrum calculated by PCM with SHARF.

A spectrum of lysozyme with Ultramark 1621 was measured for an evaluation of such influence. As shown in Fig. 7, the singly charged ions of Ultramark are observed in the *m/z* range where the multiply charged ions of lysozyme appear; thus, the peaks due to lysozyme are not easily distinguished from those of Ultramark. However, only one intense peak corresponding to the molecular mass of lysozyme is observed after the deconvolution of PCM with SHARF. The PCM order used is 5, which is slightly larger than that for the spectrum of cytochrome *c*. The influence of the singly charged ions due to Ultramark is effectively removed with the increase of the PCM order.

A mixture sample with components generating different sequences of multiply charged ions is chosen as another example. Figure 8a shows a spectrum created by co-addition of three measured spectra of cytochrome *c*, myoglobin and lysozyme. In the spectrum, the components represent different intensity distributions of the multiply charged ions: the lysozyme shows the strongest intensities with the smallest number of peaks, the myoglobin shows the weakest intensities with the largest number of peaks and the cytochrome *c* shows the middle intensities and the middle number of peaks. Figure 8b shows the result of PCM and SHARF with the PCM order of 5. The deconvoluted spectrum clearly exhibits three peaks corresponding to the components. It should be noted that the relative peak intensities in the deconvoluted spectrum of PCM depend on its order. In the PCM calculation, the absolute deconvoluted intensities are reduced with increases of the PCM order: the smaller is the number of multiply charged peaks, the larger is the reduction. In the spectrum in Fig. 8, the increases of the PCM order make the lysozyme and myoglobin intensities weaker and stronger, respectively, since the numbers of the peaks of lysozyme and myoglobin in this example are smallest and largest, respectively. If one requires true relative peak intensities, one might use the Mann method, although it generates many artifacts. Our method is useful to find the true peaks among artifact peaks, although the relative intensities are slightly damaged.

5. Conclusion

The deconvolution using the PCM and SHARF algorithms eliminates artifacts, resulting in deconvoluted spectra with good signal-to-noise ratios. Our method requires neither user-defined parameters such as a threshold level to remove influence of background noises,[6] nor *a priori* knowledge such as an intensity distribution of multiply charged ions,[5] except for the PCM order. Good deconvoluted spectra are obtained when the PCM order of 3 is applied to spectra with simple patterns, while the PCM order of 5 is applied to ones with complicated patterns. Therefore, the PCM order is not a critical parameter that is adjusted to every measured spectrum, but is a fixed parameter in most cases. If an optimal result is desired, however, the best PCM order can be found with a trial-and-error procedure, without consuming time, because a deconvoluted spectrum is quickly obtained by the effective algorithm of the deconvolution calculation.

Acknowledgment

The authors thank Mr. K. Matsuura for measuring ESI spectra and Mr. Y. Kammei for reviewing the manuscript.

References

1) T. Matsuo, R. M. Caprioli, M. L. Gross, and Y. Seyama, "Biological Mass Spectrometry," John Wiley & Sons Ltd., New York (1994).
2) J. B. Fenn, M. Mann, C. K. Meng, S. F. Wong, and C. M. Whitehouse, *Science*, **246**, 64 (1989).
3) T. R. Covey, R. F. Bonner, B. I. Shushan, and J. Henion, *Rapid Commun. Mass Spectrom.*, **2**, 249 (1988).
4) M. Mann, C. K. Meng, and J. B. Fenn, *Anal. Chem.*, **61**, 1702 (1989).
5) B. B. Reinhold and V. N. Reinhold, *J. Am. Soc. Mass Spectrom.*, **3**, 207 (1992).
6) J. J. Hagen and C. A. Monnig, *Anal. Chem.*, **66**, 1877 (1994).
7) A. G. Ferrige, M. J. Seddon, and S. A. Jarvis, *Rapid Commun. Mass Spectrom.*, **5**, 374 (1991).
8) A. G. Ferrige, M. J. Seddon, B. N. Green, S. A. Jarvis, and J. Skilling, *Rapid Commun. Mass Spectrom.*, **6**, 707 (1992).
9) Z. Zhang and A. G. Marshall, *J. Am. Soc. Mass Spectrom.*, **9**, 225 (1998).
10) K. Kokame, Y. Fukuda, T. Yoshizawa, T. Takao, and Y. Shimonishi, *Nature*, **359**, 749 (1992).
11) S. K. Chowdhury, V. Katta, R. C. Beavis, and B. T. Chait, *J. Am. Soc. Mass Spectrom.*, **1**, 382 (1990).

Keywords: Electrospray ionization, Deconvolution, Artifact elimination